10-7-2011

Parathyroid hormone and cell signaling in bone remodeling

Christina Battista

Parathyroid Hormone and Cell Signaling in Bone Remodeling

by

Christina Battista

A thesis submitted in partial fulfillment of the
requirements for the degree of Master of Science
in Applied and Computational Mathematics
from the School of Mathematical Sciences
Rochester Institute of Technology

October 7, 2011

Signature of the Author _____

Accepted by _____
Coordinator, M.S. Degree Program Date

SCHOOL OF MATHEMATICAL SCIENCES
ROCHESTER INSTITUTE OF TECHNOLOGY
ROCHESTER, NEW YORK

CERTIFICATE OF APPROVAL

M.S. DEGREE THESIS

The M.S. Degree Thesis of Christina Battista
has been examined and approved by the
thesis committee as satisfactory for the
thesis required for the M.S. degree
in Applied and Computational Mathematics

_____
Dr. David Ross, Thesis Advisor

_____
Dr. Antonio Cabal

_____
Dr. Elizabeth Cherry

_____
Dr. Christopher Wahle

_____
Date

THESIS RELEASE PERMISSION
ROCHESTER INSTITUTE OF TECHNOLOGY
SCHOOL OF MATHEMATICAL SCIENCES

Title of Thesis:

Parathyroid Hormone and Cell Signaling in Bone Remodeling

I, Christina Battista, hereby grant permission to Wallace Memorial Library of R.I.T. to reproduce my thesis in whole or in part. Any reproduction will not be for commercial use or profit.

Signature _____

Date

Parathyroid Hormone and Cell Signaling in Bone Remodeling

by

Christina Battista

Submitted to the
School of Mathematical Sciences
in partial fulfillment of the requirements
for the Master of Science Degree
in Applied and Computational Mathematics
at the Rochester Institute of Technology

Abstract

Many mathematical models relevant to osteoporosis have been developed and studied. Although osteoclasts and osteoblasts are the crucial variables in bone resorption and bone formation, PTH can cause changes in the ratio of these cells and therefore should be studied more closely. Some of the current models for osteoporosis will be analyzed in this thesis as well as amended to account for the phenomenon that occurs with various methods of PTH administration. By administering PTH in either pulsatile or continuous doses, we obtain very different results. When administered in a continuous fashion, the body experiences a net bone loss over time, but given in daily, pulsatile doses, we increase bone mineral density. By developing a model that incorporates PTH administration, we hope to provide the building block for a broader model that is able to determine the efficacy of various osteoporotic treatments.

Acknowledgments

First and foremost, I would like to express my sincere appreciation to my advisory committee: Dr. David S. Ross, Dr. Elizabeth Cherry, Dr. Antonio Cabal, and Dr. Christopher Wahle. Thank you all for providing me with guidance and support throughout this research. A special thanks goes to Dr. Ross for his time, patience, understanding, and constant advice over the past four years. You have opened my eyes to the world of applied mathematics and it has been an absolute honor to work on my thesis with you.

Thanks to the remarkable faculty and staff in the School of Mathematical Sciences who I have had the pleasure of crossing paths with in the past four years. You have taught me what it means to truly have a passion for mathematics and have allowed me to embrace my true nerdiness. I would especially like to thank Anna Fiorucci. The School of Mathematical Sciences is so privileged to have someone like you working with and touching each and every one of their students. I also want to acknowledge Dr. Joseph DeLorenzo for constantly reminding me how blessed I am and encouraging me every step of the way.

I'd also like to thank all of my friends, both at home and at RIT. Their love and patience helped me overcome many setbacks, stay focused, and have a little fun along the way. I greatly value their friendship and deeply appreciate their belief in me.

And last but definitely not least, I want to thank my mother, Carol Battista, and my older brother, Nicholas Battista. Without them I would have not made it as far as I have today. They have been there for me every step of the way, loving me unconditionally, and standing by me through all of my tough decisions.

Dedicated to my big brother, Nicky.

It was nice growing up with someone like you – someone to lean on, someone to count on ... someone to tell on.

Contents

List of Figures

Chapter 1

Introduction

Bone is living tissue, constantly adjusting its structure to provide the necessary skeletal architecture for everyday movement. The structure is adjusted by replacing old bone with newly formed bone in the process of *remodeling*. Through remodeling, the bone matrix is protected from premature deterioration and maintains its strength. Remodeling is a complex process that is the fundamental result of the interaction between osteoblasts and osteoclasts. This interaction between osteoblasts and osteoclasts is known as coupling. Osteoblasts are the cells responsible for synthesizing the bone matrix, whereas osteoclasts resorb the mineralized bone, as seen in Figure 1.1. When these cells interact in a proper way, a balance between bone gain and bone loss exists and the bone structure is maintained.

If there is a dysfunctional connection in coupling, the potential for various bone diseases arises. This dysfunctional connection could result in not enough new bone formation or in too much resorption of the mineralized bone. The most common bone disease is known as *osteoporosis*. Osteoporosis is the thinning of bone tissue and the decrease of bone density over time. (Figure 1.2) It is estimated that one in every five women over the age of fifty

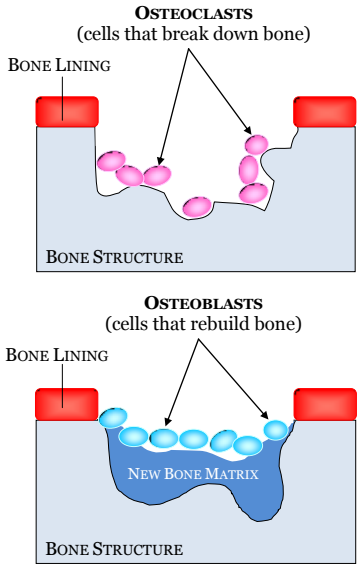

Figure 1.1: Diagram depicting the fundamental functions of osteoclasts (top) and osteoblasts (bottom); osteoblasts are responsible for constructing new bone matrix and osteoclasts resorb already existing bone.

in the United States has osteoporosis [4]. Even though only one in five are diagnosed as having osteoporosis, about half of all women over the age of fifty [4] will suffer from a severe fracture of their hip, wrist, or vertebra, the most common areas for brittle bones.

1.1 Bone Remodeling at its Core

Currently, we have discussed the basic functions of osteoblasts and osteoclasts. However, the process of becoming an active osteoblast or active osteoclast, in itself, is an intricate process (Figure 1.3).

There are several stages of cell maturation and differentiation in the osteoblastic lineage [9].

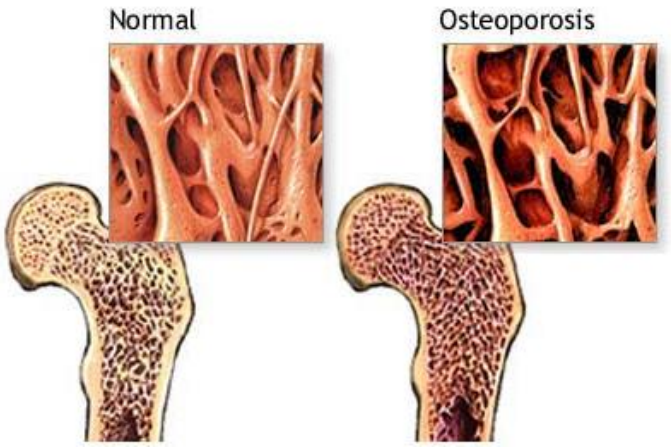

Figure 1.2: Pictorial figure showing the difference between normal and osteoporotic bones. Osteoporotic bones are more porous and therefore more vulnerable to fracture, most commonly wrist, hip, or vertebrae fractures. [4].

The source of this lineage is a collection of uncommitted mesenchymal progenitors that have the capability of becoming osteoblasts. Once these progenitors commit to the osteoblastic lineage, they enter a pool that Lemaire et al. have called *responding osteoblasts*. Although responding osteoblasts are not a specific cell type, all members of this pool share common characteristics. Through cell-to-cell contact, these responding osteoblasts are persuaded to differentiate into *active osteoblasts* under the influence of PTH and transforming growth factor beta (TGF-β)). As the active osteoclasts resorb bone, TGF-β is released from the skeleton into the bloodstream and thus stimulates osteoblastic recruitment. It should also be noted that RANKL (receptor activator of NF-κB ligand) is found on the surface of osteoblasts. RANKL will ultimately affect the osteoclastic lineage and is regulated by osteoprotegerin (OPG).

These active osteoblasts are the cells that are responsible for synthesizing new bone matter, and thus are fundamental cells in bone remodeling. However, the collection of active

osteoblasts is controlled by the pool of osteoclasts. Eventually these active osteoblasts die or transform to either lining cells or osteocytes.

Similarly, the osteoclast lineage consists of various stages beginning with hematopoietic progenitors [9]. These progenitors have RANK (receptor activator of NF-κB) on their surfaces and through cell-to-cell contact with osteoblasts, RANK and RANKL will bind, causing an increase in osteoclasts as the precursors differentiate to *active osteoclasts.* Active osteoclasts resorb bone at a rate proportional to the current number of osteoclasts. The final stage of the osteoclastic lineage is apoptosis, which is induced by TGF-β present in the bloodstream. Since TGF-β enters the bloodstream as bone is resorbed by osteoclasts, it is partly responsible for maintaining the balance between active osteoblasts and active osteoclasts. This is why more osteoclasts die when there is more TGF-β present.

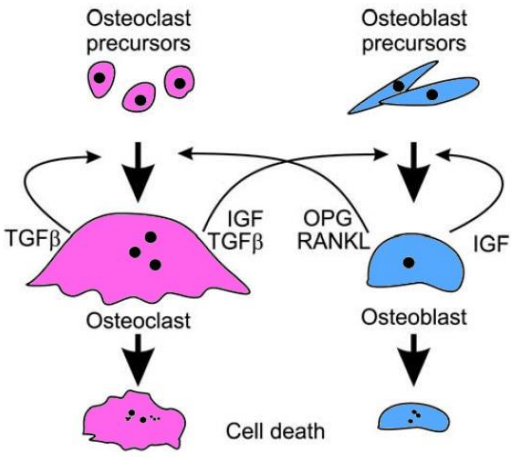

Figure 1.3: Osteoblastic and Osteoclastic Lineage [7]

1.2 Current Mathematical Models

Lemaire et al. [9] published a model of the interaction between osteoblasts and osteoclasts in bone remodeling. Lemaire et al.'s model has served as a centerpiece for this area of interest. Many others such as Peterson and Riggs [10], Raposo et al. [12], and Potter et al. [11] have studied this model as a basis for their own work. Komarova et al. [7], [6] worked parallel to Lemaire et al. and developed a model that examines the role of autocrine and paracrine regulation as it relates to osteoblast and osteoclast formation. Raposo et al. also developed a model for calcium homeostasis relating the concentrations of calcium, parathyroid hormone (PTH), and calcitriol which influence and are influenced by various glands and organs–the parathyroid, bones, kidneys, and intestines [12]. While the aforementioned models focused on the interaction of osteoblasts and osteoclasts in bone remodeling, they also incorporated parameters to account for PTH. However, when they incorporated PTH into their models, they did not include a mechanism that shows the influence of PTH on osteoblast apoptosis. This mechanism helps to demonstrate how various methods of administration play an important role in remodeling.

Kroll et al. [8] and Potter et al. [11] focused on the acknowledged effects of PTH in their models; when administered in a continuous way, PTH causes a catabolic effect, thus resulting in bone loss, but if administered in sporadic intervals, an anabolic response is evident [3]. Here, catabolic refers to the destructive process that causes a decrease in bone mineral density and anabolic refers to the the synthesis occurring in forming new bone. Bellido and co-workers have proposed a mechanism for the anabolic effect of pulsatile administration of PTH based on PTH interfering with the signaling cascade for osteoblast apoptosis [1]. We wish to also produce our own model that demonstrates the effects of PTH administration, and we look to Bellido's model for the basic idea that PTH interferes with osteoblast apoptosis. As previously stated, others have already made models that

include PTH. However, these models are not as concise as the model produced by Lemaire et al. In making a more concise model, it will allow for faster computations and ultimately be easier to incorporate into a much larger, more intricate model.

While we are working in the footsteps of Lemaire et al.'s model, we realize that their model was not intended to include the aforementioned effects of PTH. First we shall mathematically analyze the model set forth by Lemaire et al., as no one has previously done so. We will focus on proving the existence of a unique equilbrium, the bounds on the the different populations, and prove that our unique equilibrium is, in fact, a global attractor. Then we will amend the current model to incorporate equations for the signaling protein, which regulates the apoptosis rate for active osteoblasts and demonstrates this PTH phenomenon.

Chapter 2

Lemaire et al.'s Model

Lemaire et al. have set forth a concise model describing the interaction between osteoblasts and osteoclasts in bone resorption and bone formation (Figure 2.1).

2.1 The Model

As noted previously, the responding osteoblasts enter the population once progenitors commit to the osteoblastic cycle. The rate at which these progenitors commit to this particular cycle is dependent upon the current concentration of active osteoclasts. Since these osteoclasts release calcium and TGF-β into the bloodstream, the osteoclast population has a strong control on the number of responding osteoblasts. However, the responding osteoblast population only loses members through differentiation into active osteoblasts. This rate is also determined by the amount of TGF-β in the bloodstream. Since our body needs to maintain a balance (as to prevent diseases such as osteoporosis) more active osteoblasts must be produced to aid in this balance, thus diminishing the responding osteoblast population.

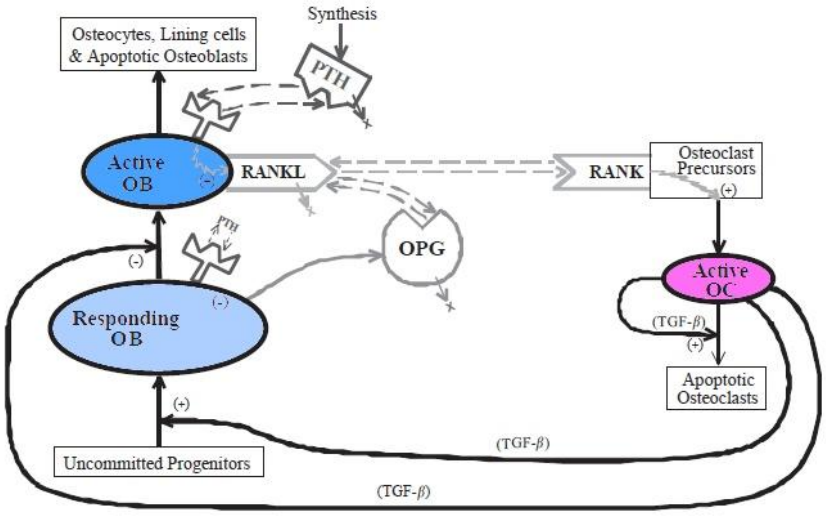

Figure 2.1: Diagram representing the basic structure of Lemaire et al.'s model [9]. It depicts how certain cell types interact with other cells and the chemicals given off or needed in the process of specific cell lineages. The dark solid lines represent the interaction of cells, whereas the light solid lines show the chemicals given off by typical cell functions. The dashed lines show the bonds formed between chemicals.

Thus, differentiation from responding osteoblasts is the only source for increase in the active osteoblast pool. Similarly, active osteoclasts are created when they differentiate from their precursor stages. The osteoclast lineage consists of at least four different types of cells, beginning with the precursors and culminating in active osteoclasts. Lemaire et al. have chosen not to include the precursor or responding osteoclast stages in their model because it would cause a drastic increase in the complexity of the model and they sought to create a concise, simplistic model.

Both active osteoblasts and active osteoclasts experience apoptosis and die at a natural rate, thus removing members of each class respectively. Clearly, their death rates rely upon

the current number of their members. However, the population of the opposing cells also affects this rate. In Lemaire et al.'s model, it is assumed that responding osteoblasts do not experience apoptosis. They must differentiate into active osteoblasts, thus differentiation is the only way the responding osteoblast population loses members. For the purposes of Lemaire et al.'s model, it should be noted that there is no movement from osteocytes to osteoblasts. In other words, once a cell has left the active osteoblast collection, it is no longer capable of forming new bone and thus leaves our model completely.

With the interactions described in the above paragraphs, Lemaire et al. have created a system of differential equations accounting for the interaction between each of these cell populations in time units of days:

$$\frac{dR}{dt} = D_R\pi_C - \frac{D_B}{\pi_C}R \tag{2.1}$$

$$\frac{dB}{dt} = \frac{D_B}{\pi_C}R - k_B B \tag{2.2}$$

$$\frac{dC}{dt} = D_C\pi_L - D_A\pi_C C \tag{2.3}$$

where $D_B = f_0 \cdot d_B$, $\pi_C(C) = \frac{C+f_0C^s}{C+C^s}$, and $\pi_L(R,B) = \frac{k_3}{k_4} \cdot \frac{K_L^P \pi_P B}{1+\frac{k_3K}{k_4}+\frac{k_1}{k_2k_O}\cdot(\frac{K_O^P}{\pi_P}R+I_O)} \cdot (1+\frac{I_L}{r_L})$. The term π_P represents the fraction of occupied PTH receptors given by $\pi_P = \frac{\bar{P}+P^0}{\bar{P}+P^s}$ with $\bar{P} = \frac{I_P}{k_P}$, $P^0 = \frac{S_P}{k_P}$, and $P^s = \frac{k_6}{k_5}$.

This model clearly has many variables and parameters which are defined as follows with the corresponding units in parenthesis:

- $R(t)$: the concentration of responding osteoblasts at time t (pM)
- $B(t)$: the concentration of active osteoblasts at time t (pM)
- $C(t)$: the concentration of active osteoclasts at time t (pM)
- C^s : the value of C to get half differentiation flux (pM)

- ⋆ D_A : the rate of osteoclast apoptosis caused by TGF-β (day^{-1})
- ⋆ d_B : the differentiation rate of responding osteoblasts (day^{-1})
- ⋆ D_C : the differentiation rate of osteoclast precursors (pM day^{-1})
- ⋆ D_R : the differentiation rate of osteoblast progenitors (pM day^{-1})
- ⋆ f_0 : fixed proportion (no units)
- ⋆ I_L : the rate of administration of RANKL (pM day^{-1})
- ⋆ I_O : the rate of administration of OPG (pM day^{-1})
- ⋆ I_P : the rate of administration of PTH (pM day^{-1})
- ⋆ K : fixed concentration of RANK (pM)
- ⋆ k_1 : the rate of OPG-RANKL binding (pM^{-1} day^{-1})
- ⋆ k_2 : the rate of OPG-RANKL unbinding (day^{-1})
- ⋆ k_3 : the rate of RANK-RANKL binding (pM^{-1} day^{-1})
- ⋆ k_4 : the rate of RANK-RANKL unbinding (day^{-1})
- ⋆ k_5 : the rate of PTH binding with its receptor (pM^{-1} day^{-1})
- ⋆ k_6 : the rate of PTH unbinding (day^{-1})
- ⋆ k_B : the rate of elimination of active osteoblasts through apoptosis (day^{-1})
- ⋆ K_L^P : the maximum number of RANKL attached on cell surface (pmol/pmol cells)
- ⋆ k_O : the rate of elimination of OPG (day^{-1})
- ⋆ K_O^P : the minimal rate of production of OPG per cell (pmol day^{-1}/pmol cells)

- ⋆ k_P : the rate of elimination of PTH (day^{-1})
- ⋆ r_L : the rate of RANKL production and elimination (pM day^{-1})
- ⋆ S_P : the rate of synthesis of systemic PTH (pM day^{-1})

The values of the aforementioned parameters can be found in Appendix A. For simplicity, we will write π_L as $\frac{\sigma B}{\gamma+R}$ where $\sigma = \frac{k_3}{k_4}\cdot\frac{k_L^P\pi_P k_2 k_0 \pi_P}{k_1 k_O^P}\cdot(1+\frac{I_L}{r_L})$ and $\gamma = (1+\frac{k_3 K}{k_4}+\frac{k_1 I_O}{k_2 k_O})\cdot\frac{k_2 k_O \pi_P}{k_1 k_O^P}$, both of which are positive values. For the purposes of the following proofs, note that all parameter values are nonnegative.

2.2 Analysis of the Model

Since no one has previously analyzed Lemaire's system, we will perform a mathematical analysis and provide proofs that correspond to the claims stated in their work. Lemaire et al. have stated that their system admits only one fixed point (equilibrium) in the parameter space and that this point is stable. In this thesis, we will focus on proving the existence of a unique equilibrium, the bounds on the the different populations, and prove that our unique equilibrium is, in fact, a global attractor. In the process of doing so, we will also perform a local linear analysis of the system.

2.2.1 Local Linear Analysis of the Model

Although we wish to prove that the equilibrium is a global attractor, we will perform a local analysis to ensure that at the local level, our equilibrium is, in fact, a sink. In order to perform a local analysis, we must first find the Jacobian matrix and then evaluate it at our equilibrium point $(R, B, C) = (0.0007734, 0.0007282, 0.0009127)$ (all in pM). Our

Jacobian matrix will take on the following form

$$\begin{pmatrix} \frac{\partial \dot{R}}{\partial R} & \frac{\partial \dot{R}}{\partial B} & \frac{\partial \dot{R}}{\partial C} \\ \frac{\partial \dot{B}}{\partial R} & \frac{\partial \dot{B}}{\partial B} & \frac{\partial \dot{B}}{\partial C} \\ \frac{\partial \dot{C}}{\partial R} & \frac{\partial \dot{C}}{\partial B} & \frac{\partial \dot{C}}{\partial C} \end{pmatrix}$$

Case I: π_C and π_L as Constants

Since our system is nonlinear, we will first consider the linear case where π_C and π_L are constant. This system is irrelevant to the biological model, but this may help with the analysis of the nonlinear model. In the case where π_C and π_L are constant, the Jacobian can be easily found.

$$\begin{pmatrix} -\frac{D_B}{\pi_C} & 0 & 0 \\ \frac{D_B}{\pi_C} & -k_B & 0 \\ 0 & 0 & -D_A\pi_C \end{pmatrix}$$

The above matrix is clearly a constant lower triangular matrix, which means the eigenvalues are simply the entries along the diagonal. Our eigenvalues are then $-\frac{D_B}{\pi_C}$, $-k_B$, and $-D_A\pi_C$. Because all of our parameter values are positive, it is obvious that these three entries are all negative for any given equilibrium. Thus, when considering the case of constant values for π_C and π_L, our system is a sink and therefore locally stable.

Case II: π_C and π_L as Functions

Although the above linearization was simple, it unfortunately does not prove anything about the realistic system we are dealing with. We must find the Jacobian in the case where π_C and π_L are not constants and evaluate it at the aforementioned equilibrium point. Due to the nonlinearity of our system, our Jacobian looks much more complex

than the previous.

$$\begin{pmatrix} -\frac{D_B}{\pi_C} & 0 & D_R\pi_C{}' + \frac{D_B R\pi_C{}'}{\pi_C^2} \\ \frac{D_B}{\pi_C} & -k_B & -\frac{D_B R\pi_C{}'}{\pi_C^2} \\ -\frac{D_C B\sigma}{(\gamma+R)^2} & \frac{D_C\sigma}{\gamma+R} & -(D_A\pi_C + D_A C\pi_C{}') \end{pmatrix}$$

where

$$\pi_C{}' = \frac{C^s(1+f_0)}{(C+C^s)^2}.$$

Because of the nonlinear nature of this matrix, it was extremely difficult to find the eigenvalues analytically. Instead, we opted to find them numerically once we evaluated the matrix at the system's equilibrium point. We knew the values of all the parameters with the exception of f_0. Varying the value of f_0 causes a drastic change in the eigenvalues. Although all eigenvalues have a negative real parts, some values of f_0 would give us three real eigenvalues while others would give us one real eigenvalue and two imaginary eigenvalues.

When we attempted to find the point of bifurcation, it was not as simple as expected. It doesn't seem as though there is a set limit for f_0 for which the eigenvalues go from being all real to being mixed between real and imaginary values. However, all eigenvalues had a negative real part, thus showing that our equilibrium is locally stable. There is currently no proof to show that this is true, however.

We can see in Figure 2.2 that although we change our initial values quite drastically, we still end up at the same equilibrium point in all three cases presented here. This leads us to believe that our system is a global attractor. The following analysis provides the basis for a global attractor proof.

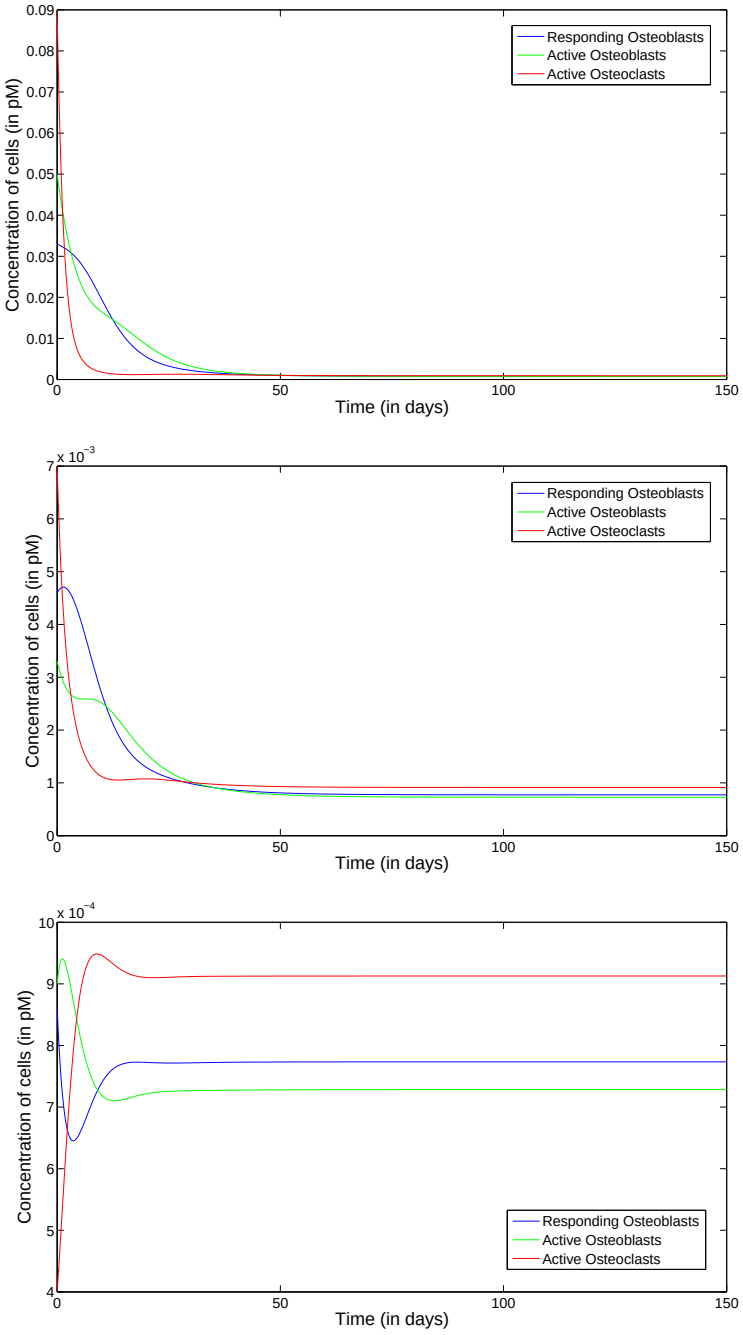

Figure 2.2: Graphs of the numerical solution to Lemaire et al.'s model at various initial conditions $[R_0, B_0, C_0]$: $[0.033, 0.05, 0.09]$ (top), $[0.0046, 0.0033, 0.007]$ (middle), $[0.00086, 0.0009, 0.0004]$ (bottom). As the initial values vary, we still find the same equilibrium point, giving reason to believe there exists a unique equilibrium.

2.2.2 Bounds on Variables

Positivity

Since this model represents a realistic scenario, we wish for its limits to also maintain realistic values. Thus, we want to prove that this model maintains realistic, positive values for all positive initial conditions.

Theorem 1. *If R_0, B_0, $C_0 > 0$, then $R(t)$, $B(t)$, $C(t) > 0$ for all t where $R(0) = R_0$, $B(0) = B_0$, and $C(0) = C_0$.*

Proof. Assume there exists $T > 0$, where T is the smallest value of t for which at least one of the following is true:

- $R(t) = 0$
- $B(t) = 0$
- $C(t) = 0$

where $0 < f_0 \leq \pi_C \leq 1$. This inequality follows directly from $\pi_C(C) = \frac{C+f_0C^s}{C+C^s}$ as $0 \leq C < \infty$.

First, assume $R(t) = 0$ at $t = T$. Then $\frac{dR}{dt} = D_R\pi_C \geq D_Rf_0 > 0$. Since $R_0 > 0$ and $\frac{dR}{dt} > 0$ for all $t < T$, there exists $\varepsilon > 0$ such that $\frac{dR}{dt} > \frac{D_Rf_0}{2}$ for $T - \varepsilon < t < T + \varepsilon$. On this interval, $R(t) > 0$ and $\frac{dR}{dt} > \frac{D_Rf_0}{2}$ so it follows that $R(T) - R(t) > \frac{D_Rf_0}{2}(T - t)$. Rearranging this, we find that $R(T) > R(t) + \frac{D_Rf_0}{2}(T - t) > R(t)$. Thus, $R(T) > R(t)$ and we have that $R(t) \neq 0$ for any value of t.
Using the above bounds for $R(t)$, we can then find bounds for $B(t)$ followed by bounds for $C(t)$.

Therefore, Lemaire's system is restricted to the positive octant, given nonnegative initial values. ■

2.2.3 Unique Equilibrium

As previously mentioned it can be helpful to first consider the case in which π_C and π_L are constants. In this case, the equilibrium exists at

$$(R, B, C) = \left(\frac{D_R \pi_C^2}{D_B}, \frac{D_R \pi_C}{k_B}, \frac{D_C \pi_L}{D_A \pi_C} \right).$$

However, in the realistic case where π_C and π_L are not constants, we wish to prove that there is a unique equilibrium solution and eventually that it is a global attractor. Again, we will write π_L as $\frac{\sigma B}{\gamma + R}$ where $\sigma = \frac{k_3}{k_4} \cdot \frac{k_L^P \pi_P k_2 k_0 \pi_P}{k_1 k_O^P} \cdot (1 + \frac{I_L}{r_L})$ and $\gamma = (1 + \frac{k_3 K}{k_4} + \frac{k_1 I_O}{k_2 k_O}) \cdot \frac{k_2 k_O \pi_P}{k_1 k_O^P}$, both of which are positive values.

Theorem 1. *There exists a single, unique equilibrium in the dynamical system defined by Equations* (2.1)*,* (2.2)*, and* (2.3)*.*

Proof. Since the equilibrium in the constant case depended upon π_C, the equilibrium points for R and B become functions of π_C in the realistic scenario.

$$R = \frac{D_R \pi_C^2}{D_B} \text{ and } B = \frac{D_R \pi_C}{k_B}$$

Since π_C is a function of C we must solve for the equilibrium of C using the above equilibrium points for R and B:

$$\begin{aligned} \frac{dC}{dt} &= D_C \pi_L - D_A \pi_C C \\ &= \frac{D_C \sigma D_B D_R}{k_B (D_B \gamma + D_R \pi_C^2)} - D_a C \end{aligned}$$

Setting the above equation equal to zero and solving for C will give us the equilibrium.

$$\Rightarrow C = \frac{D_C \sigma D_B D_R}{D_A k_B (D_B \gamma + D_R \pi_C^2)}$$

Define a new function,

$$F(C) = C - \frac{D_C \sigma D_B D_R}{D_A k_B (D_B \gamma + D_R \pi_C^2)}.$$

We can now study this $F(C)$ equation further to help us determine equilibrium solutions. Since we have previously proven that C is bounded below by zero, we must study $F(C)$ for only nonnegative values of C. If we can prove that $F(C) = 0$ for one and only one value of C, then it follows that R and B both also only have one value since they functions of C.

We find that $F(0) = -\frac{D_C D_R D_B \sigma}{D_A k_B D_B \gamma + D_A k_B D_R \pi_C^2} < 0$ and $\lim_{C \to \infty} F(C) = \infty$. Since this function starts as a negative value and is continuous to ∞, it is necessary to prove that $F(C) = 0$ at some value of C. In other words, we wish to show that $F(C)$ is a strictly increasing function.

$$F'(C) = 1 + 2\frac{D_C D_R^2 D_B D_A k_B \pi_C \pi_C' \sigma}{(D_A k_B (D_B \gamma + D_R \pi_C^2))^2} \geq 1$$

This is sufficient to show that $F(C)$ is a strictly increasing function. Since we know that $F(C)$ is negative for small values of C and strictly increasing to ∞, $F(C)$ must equal zero at one and only one value of C.

Thus, there exists a single equilibrium point for our system. ■

2.2.4 Global Attractor

Although I haven't yet proven the equilibrium to be a global attractor, I have made progress towards finding such a proof and have shown various methods that are not useful

for this system.

Some methods have been tried in proving it to be a global attractor.

- ⋆ I have tried to find an appropriate Lyapunov function for Lemaire's dynamical system.
- ⋆ I turned the nonlinear system into a system of polynomials to make it easier to manage.
  - I, again, tried to find the Lyapunov function for the system of polynomials.
- ⋆ I began working on a "Nested Box" method [13].

Collaborative work with several colleagues has resulted in the developed proof continuing off of the "boxing-in" method. This proof will appear in a paper to be published later by Ross, Battista, Cabal, and Mehta [14].

2.2.5 Numerical Results

We implemented this system in `MATLAB` using the built-in `ode45` function. We compared our results to those of Lemaire's in order to check that our code was working properly before moving on with this research. Using the same values presented by Lemaire, we were able to reconstruct the exact graphs from their paper (Figure 2.3). This `ode45` function uses a Runge-Kutta method with a variable time-step to find the best solution. Using this function, we set an error tolerance of 10^{-9} to obtain the best results possible. The values of the parameters using during numerical trials can be found in Appendix A. Also, from this code we were able to determine the "average" osteoclast/osteoblast (OC/OB) ratio which we will use later to determine the effects from incorporating PTH into our model. The typical OC/OB ratio is found to be 1.248 so we expect to find a higher ratio

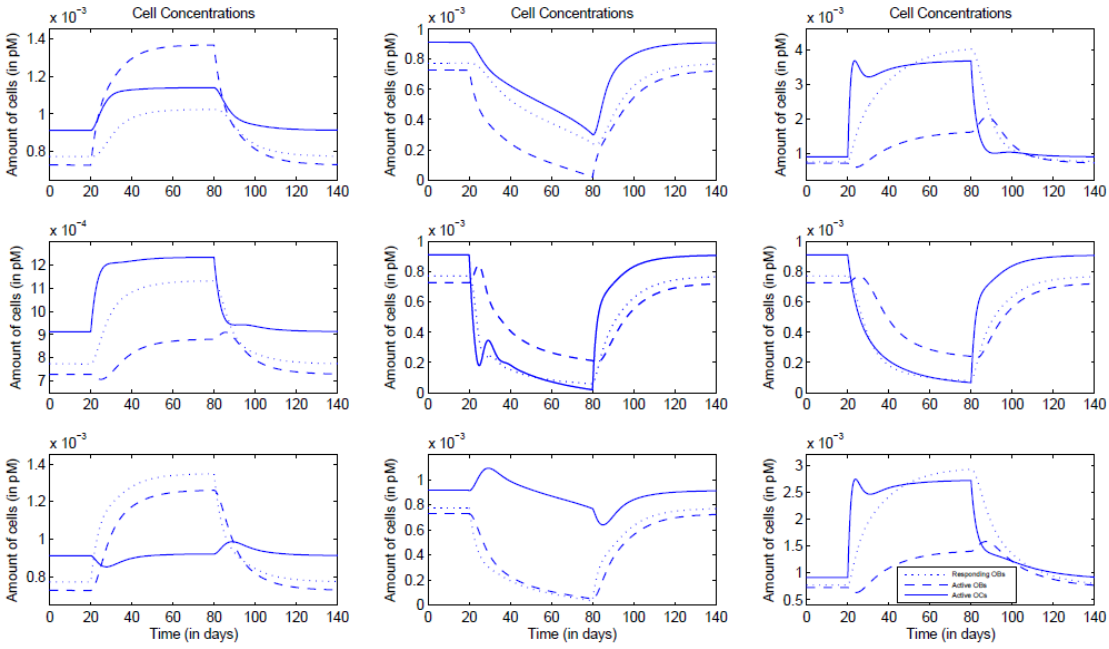

Figure 2.3: Reconstructed graphs from Lemaire's paper using our `MATLAB` code

when administering PTH in a continuous fashion and a lower ratio when administering it in daily pulses. The OC/OB ratio is commonly thought of as an indicator for bone loss/bone gain. As the ratio varies from 1.248, we can determine if more resorption is occurring (which could lead to bone diseases) or more bone formation is occurring.

Chapter 3

Signaling Protein Model

Parathyroid hormone (PTH) plays a crucial role in bone remodeling. This is the motivation for my studying the effects of PTH. When looking at the effects of osteoporosis, it would be beneficial to determine if PTH could somehow improve bone mineral density for those affected by this disease. Since many pharmaceutical companies are concerned with the effects of PTH in bone remodeling, it is important to demonstrate the phenomenon that occurs when PTH is administered in different ways. Bellido and co-workers have proposed a mechanism for the anabolic effect of pulsatile administration of PTH based on PTH interfering with the signaling cascade for osteoblast apoptosis [1]. In our model, we add in a signaling protein, similar to Bellido et al., which controls the apoptosis rate for the active osteoblasts under the influence of PTH in the bloodstream. In order to exhibit the phenomenon that occurs when administering PTH in various manners, we will amend the previous model provided by Lemaire et al.

3.1 The Model

Our model has the same basic parameters as Lemaire et al.'s model with a few additional parameters. The most obvious alteration is the addition of two differential equations representing the signaling protein and a signaling protein/PTH complex, respectively.

The signaling protein, $S(t)$, is added into our model to control the apoptosis rate of active osteoblasts. If more of the signaling protein is present, we have a higher apoptosis rate for osteoblasts. Clearly a lower concentration of signaling protein in the bloodstream causes a slower rate of death for active osteoblasts. As signaling protein varies in concentration, it is obvious that a direct relationship exists between the amount of signaling protein and the signaling protein/PTH complex, $Q(t)$.

Our signaling protein model is as follows:

$$\frac{dR}{dt} = D_R\pi_C - \frac{D_B}{\pi_C}R \tag{3.1}$$

$$\frac{dB}{dt} = \frac{D_B}{\pi_C}R - k_B\frac{e^{\lambda(S-1)}}{a+be^{\lambda(S-1)}}B \tag{3.2}$$

$$\frac{dC}{dt} = D_C\pi_L - D_A\pi_C C \tag{3.3}$$

$$\frac{dS}{dt} = k_S(1-S) - k_f P(t)S + k_R Q \tag{3.4}$$

$$\frac{dQ}{dt} = k_f P(t)S - k_R Q \tag{3.5}$$

where π_C and π_L are defined as above in Chapter 2. However, we now let

$$\pi_P = \frac{P(t)+P^0}{P(t)+P^s}$$

with $P^0 = \frac{S_P}{k_P}$, $P^s = \frac{k_6}{k_5}$, and $P(t)$, a function with value greater than the value of $\bar{P}$ previously used in Lemaire et al.'s model. This $P(t)$ function represents the administration of PTH. PTH is administered in the form of teriparatide, an osteoporosis treatment. Because π_P becomes a function of $P(t)$ in this model and σ and γ were both dependent

on π_P in Lemaire et al.'s model, σ and γ must also become functions of $P(t)$. Recall that $\pi_L = \frac{\sigma B}{\gamma + R}$. Thus, π_L is also a function of $P(t)$.

We have also added the following parameters: k_S, k_f, and k_R. k_S is the rate at which the signaling protein equilibrates, k_f is the binding rate for the signaling protein and PTH, and k_R is the unbinding rate for the signaling protein/PTH complex.

We can now control the rate and type of administration of PTH into the bloodstream by altering the function that represents $P(t)$. For the purposes of this thesis, we sought out functions of $P(t)$ that would resemble the results found by Cosman et al. [2] in order to experience an anabolic effect on bone mineral density. However, we also wanted to demonstrate what occurs when PTH is administered in various ways. For this reason, we will use both $P(t)$ functions that strongly resemble those presented by Cosman et al. as well as functions that represent a continuous administration of PTH to the bloodstream. If we were to let $P(t) = 0$, we obtain the same results as those found using the model provided by Lemaire et al.

3.2 Relevant Data

Cosman et al. have provided a detailed description of their findings through purely experimental evidence [2]. They successfully enrolled 155 postmenopausal women (64 years or older) into this experiment, separating them into five groups over the six month period. The groups were broken down by administration of teriparatide into the following categories:

- ⋆ a teriparatide patch with a $20 - \mu$g dose
- ⋆ a teriparatide patch with a $30 - \mu$g dose

- ⋆ a teriparatide patch with a $40 - \mu$g dose
- ⋆ a $20 - \mu$g dose of teriparatide that was injected daily, and
- ⋆ a placebo.

The transdermal patch was a new idea that hoped to provide the rapid pulse that would produce the desired outcome.

In their study, they found that the transdermal patch of teriparatide in postmenopausal women with osteoporosis was safe and effective in increasing total hip and lumbar spine bone mineral density over a six month period.

Along with Cosman et al., Finkelstein et al. had performed a similar experiment [5]. In their experiment, they administered teriparatide (PTH) to both osteoporotic men and women once daily. They administered PTH to their patients initially in months 6-30, withdrew them from treatment for months 30-42, and began treatment again in months 42-54. Their results can be summarized in Figure 3.1.

Although they have shown an increase in bone mineral density, their experiments have yet to show that this also causes a decreased likelihood of fracture. It is a common conception that an increase in bone mineral density will eventually reduce the risk or fracture, but their experiment specifically set out to show an increase in bone mineral density and not make any statements about the risk of fracture.

3.3 Numerical Results

We developed the appropriate $P(t)$ functions we were searching for and incorporated them into our five-equation system to find the expected results. When placing these functions

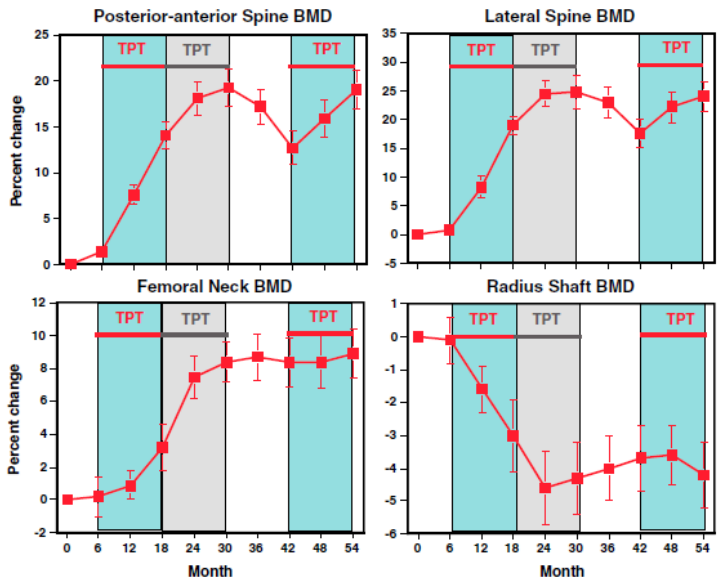

Figure 3.1: The results of Finkelstein et al. showing change in bone mineral density of the posterior-anterior spine, lateral spine, femoral neck, and radius shaft during the various stages of their treatment, withdrawal, and re-treatment experiment. [5]

into our system, we also had to seek out parameter values which contributed to the correct results. It should be noted that the parameter values we used were chosen purely because they produced the desired results. Our system, with the new parameter values becomes

$$\frac{dR}{dt} = D_R\pi_C - \frac{D_B}{\pi_C}R \tag{3.6}$$

$$\frac{dB}{dt} = \frac{D_B}{\pi_C}R - k_B\frac{e^{150(S-1)}}{\frac{1}{6}+\frac{5}{6}e^{150(S-1)}}B \tag{3.7}$$

$$\frac{dC}{dt} = D_C\pi_L - D_A\pi_C C \tag{3.8}$$

$$\frac{dS}{dt} = 1.5(1-S) - 0.19P(t)S + 0.719Q \tag{3.9}$$

$$\frac{dQ}{dt} = 0.19P(t)S - 0.719Q. \tag{3.10}$$

Most importantly, when separating continuous and pulsatile administration, it was necessary to ensure that we maintain the same cumulative dose over a daily 24-hour period. This ensures that patients receive the same amount of PTH (thus eliminating the amount administered from being the cause of a change) and proving that the method of administration is, in fact, the determining factor for anabolic/catabolic results.

3.3.1 Constant Administration of PTH

When modeling the system with a constant adminstration of PTH, we used the function (Figure 3.2)

$$P(t) = \frac{S_p}{k_p} + 350\frac{\sqrt{\pi}}{2*37^{3/2}}. \tag{3.11}$$

With the above PTH function and given parameter values, we obtain an average OC/OB ratio of 1.397, which is clearly higher than the stable ratio of approximately 1.248. Our graph ends up looking similar to that of Lemaire et al.'s model with just a higher OC/OB ratio (Figure 3.3). This causes a net bone resorption.

This net bone resorption can be mathematically explained. While $P(t)$ is a constant,

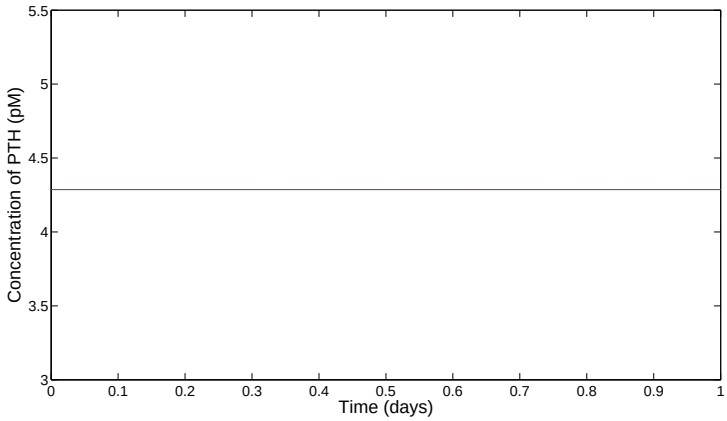

Figure 3.2: Our function $P(t)$ for continuous administration of PTH over one day

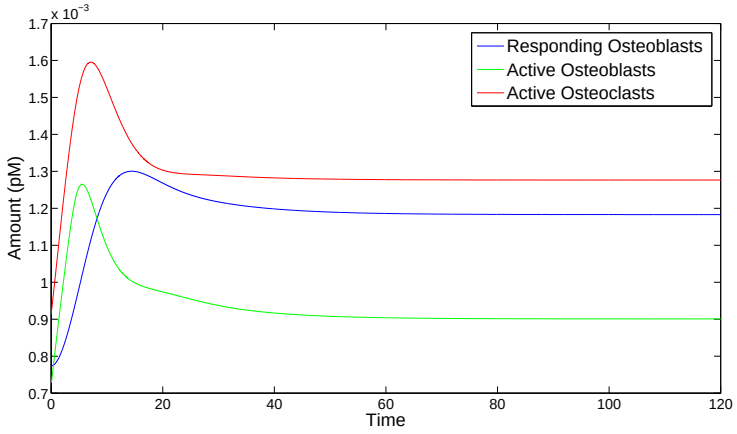

Figure 3.3: Results of our system with a continuous administration of PTH

equations (3.4) and (3.5) become linear functions where we can find the equilibrium to be $S = 1$ and $Q = \frac{k_f P(0)}{k_R}$. As an extension of the global attractor proof provided by Ross et al. when dealing with Lemaire's system, this equilibrium can also be shown to be a global attractor (although it will not be shown in this thesis.) As the baseline of PTH increases to the constant $P(t)$, it alters the concentrations of both osteoblasts and osteoclasts, and then settles the signaling protein concentration to its baseline value. As it approaches the signaling protein baseline value, the PTH level is still increased and thus a higher OC/OB ratio occurs.

3.3.2 Pulsed Administration of PTH

Again, when we were in search of a function for the pulsed PTH administration, we referenced the graphs that Cosman et al. had produced from their experiment [2]. Note that their graph has different scalings so our values look different, but if converted to the same units our graph matches theirs rather well. We use the function (Figure 3.4)

$$P(t) = \frac{S_p}{k_p} + 350\sqrt{t}e^{-37t}. \tag{3.12}$$

In order to administer a pulse each morning, we use a modulus function to alter the time so a pulse is given just once a day and it repeats the same pulse each following day. Using this method and the above equation for pulsatile PTH administration, we find the results we expected; the OC/OB ratio is lower, causing a net increase in bone mineral density (Figure 3.5).

When we use this pulsatile method of PTH administration, the entire signaling protein dynamical system must oscillate daily. As this system oscillates, it is clear that the signaling protein concentration must also oscillate and in doing so, causes the apoptosis rate $\frac{e^{\lambda(S-1)}}{a+be^{\lambda(S-1)}}$ to respond differently with various concentrations of signaling protein. With lower concentrations, the apoptosis rate reacts more actively than with higher concen-

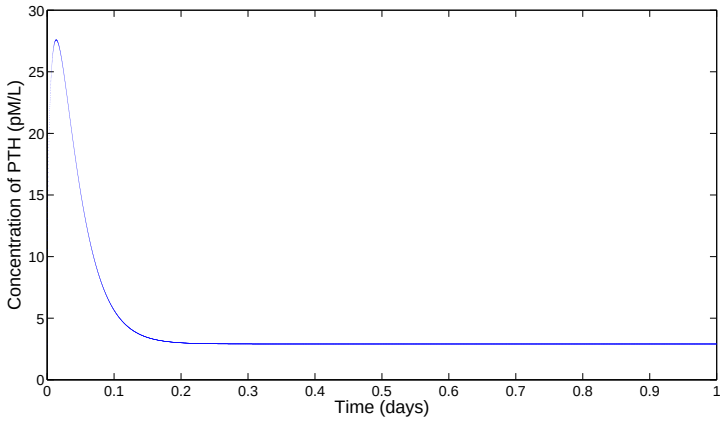

Figure 3.4: Our function $P(t)$ for pulsatile administration of PTH over one day

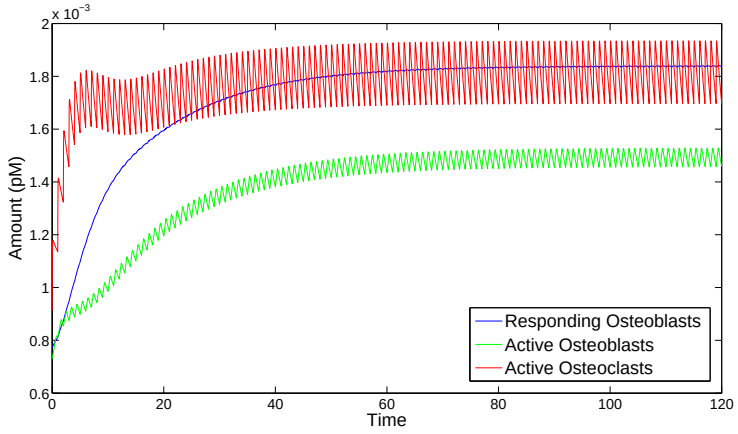

Figure 3.5: Results of our system with a pulsatile administration of PTH

trations of signaling protein. This results in a higher concentration of osteoblasts than osteoclasts and therefore the OC/OB ratio decreases.

3.3.3 No PTH Administration

When there is no administration of parathyroid hormone, we obtain the same results found in Lemaire et al.'s model, as expected. The OC/OB ratio is still approximately 1.248, and the same equilibrium is found in this case.

3.4 Bone Mineral Density

I have proposed the addition of another equation relating to our system. This additional equation represents bone mineral density (BMD) as a percent of the baseline and is defined as

$$\frac{dBMD}{dt} = \kappa(1.25\frac{B}{C} - 1) \tag{3.13}$$

where 1.25 comes from the "normal" OC/OB ratio and κ is simply a fixed proportion to obtain accurate results. Because osteoblasts and osteoclasts are the main components in bone formation/resorption, we have chosen to base our bone mineral density off of solely their values.

However, I realize the simplicity of this equation and for future work, it would be beneficial to more accurately develop this equation. For the purposes of this thesis, we will use this equation as a rough outlook at the BMD for our two cases. Selecting κ to be 0.005, we have found a simpler way of displaying the increase/decrease in bone mineral density. Figures 3.6 and 3.7 show the change in BMD over a 2-year period with pulsatile and continuous administration of teraparitide.

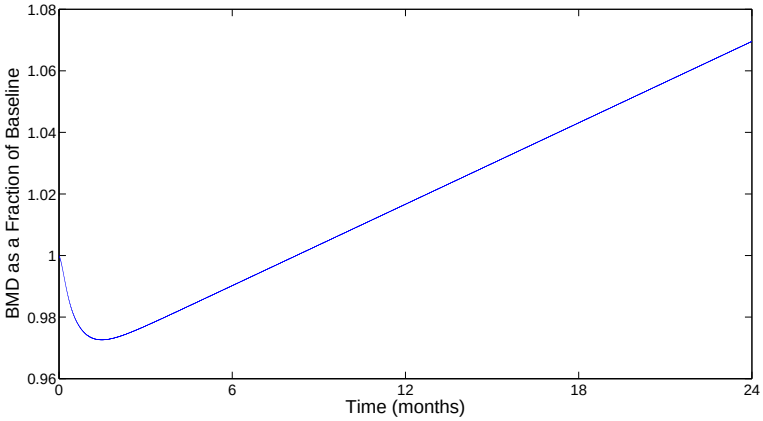

Figure 3.6: Bone mineral density over a 2-year period with daily pulsatile administration of PTH

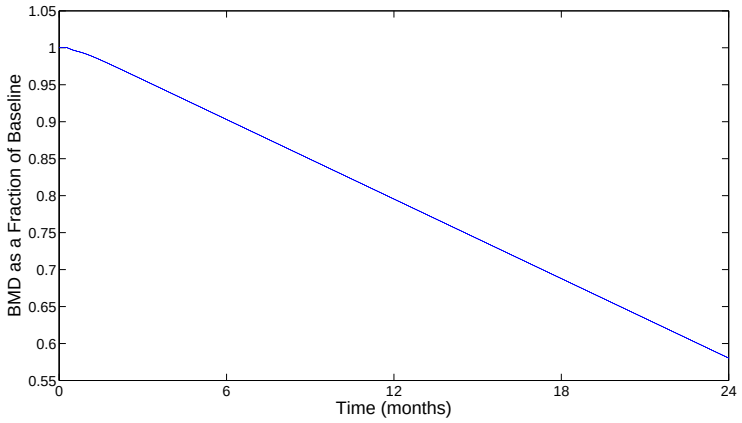

Figure 3.7: Bone mineral density over a 2-year period with continuous administration of PTH

If we look at other results featured in Cosman et al.'s paper, we find that our increase in bone mineral density in the hip and lumbar spine matches their data rather well [2]. Other areas of the body, however, do not seem to fit our model as well. These parts of the body that do not match our results might be a better fit with other values of κ.

Chapter 4

Conclusion

In this thesis, we have done some analysis on Lemaire et al.'s model and determined that not only does it represent biological information correctly, but it also coincides with the laws of mathematics; given realistic initial conditions, we have proven that our solution will always be a unique, realistic solution and we have set up the beginnings to prove that our equilibrium is actually a global attractor. Lemaire et al. have successfully captured the interaction of osteoblasts and osteoclasts in bone remodeling, which was their main focus. Not only did their model provide a foundation by which we could verify the accuracy of our `MATLAB` code, but it also provided the basis for our expanded dynamical system which incorporated various methods of PTH administration.

Also, from the mathematical structure of our model, we were able to mathematically determine how the various administration methods for PTH produce different results. This was one of our main goals that we set out to do in the beginning. Many people such as Bellido et al., were aware of the effects of different PTH administration techniques, but previously the cause of these effects was not discussed. We have represented the outcome numerically as well as discussed a short proposition as to why a particular outcome occurs.

4.1 Future Work

Although we have constructed a model which correctly depicts the qualitative anabolic/catabolic effects based on PTH administration, there is still more research to be performed behind this model. Firstly, it must be further researched to determine if the parameters we have chosen are actually good fits for the biological model, not just fitting the desired outcome. These parameter values must be consistent with the biological happenings behind the model, rather than chosen arbitrarily as we have done. Since these parameters were chosen arbitrarily, our system agrees qualitatively, but not necessarily quantitatively. In choosing biologically-relevant parameter values, our model might match the data better quantitatively.

In addition to verifying parameter values, one might also want to consider defining different PTH functions to mimic more of those found in Cosman's experiment. As we have seen, our model fits the $20 - \mu$g treatment, but other PTH functions could be found to fit the other treatments as well. Along with this, we could study the impact (if any) that the shapes of these PTH functions play on bone mineral density.

Lastly, our work could be expanded into a broader model that incorporates Lemaire et al.'s model, our model, BMD, and other elements that can be used to evaluate the efficacy of various osteoporotic treatments.

Appendix A

Parameter Values

Symbol	Value	Units
C^s	5×10^{-3}	pM
D_A	0.7	day^{-1}
d_B	0.7	day^{-1}
D_C	2.1×10^{-3}	pM day^{-1}
D_R	7×10^{-4}	pM day^{-1}
f_0	0.05	No dimension
I_L	$0 - 10^6$	pM day^{-1}
I_O	$0 - 10^6$	pM day^{-1}
I_P	$0 - 10^6$	pM day^{-1}
K	10	pM
k_1	10^{-2}	pM^{-1} day^{-1}
k_2	10	day^{-1}
k_3	5.8×10^{-4}	pM^{-1} day^{-1}
k_4	1.7×10^{-2}	day^{-1}
k_5	0.02	pM^{-1} day^{-1}
k_6	3	day^{-1}
k_B	0.189	day^{-1}
K_L^P	3×10^6	pmol/pmol cells
k_O	0.35	day^{-1}
K_O^P	2×10^5	pmol day^{-1}/pmol cells
k_P	86	day^{-1}
r_L	10^3	pM day^{-1}
S_P	250	pM day^{-1}

Appendix B

Code for Lemaire's Model

```
function osteo(t, y)

R0 = 0.0007734;
B0 = 0.0007282;
C0 = 0.0009127;

Tstop = 100;

[T,Y] = ode45(@program5,[0 Tstop], [R0 B0 C0]);

x1 = Y(:,1);
x2 = Y(:,2);
x3 = Y(:,3);

figure(1);clf;
plot(T, x1,'b');
```

```
xlabel('Time');
ylabel('Responding Osteoblasts');
hold on;

plot(T, x2,'g');
xlabel('Time');
ylabel('Active Osteoblasts');

hold on;
plot(T, x3,'r');
xlabel('Time');
ylabel('Active Osteoclasts');

x1(end)
x2(end)
x3(end)

return


function yp = program5(t,y)

RR=y(1);
BB=y(2);
CC=y(3);

Cs = 5e-3;
```

```
Da = 0.7;
db = 0.7;
Dc = 2.1e-3;
Dr = 7e-4;
f0 = 0.15;
IL = 0;
I0 = 0;
Ip = 0;
K = 10;
k1 = 1e-2;
k2 = 10;
k3 = 5.8e-4;
k4 = 1.7e-2;
k5 = 0.02;
k6 = 3;
kb = 0.189;
klp = 3e6;
k0 = 0.35;
kop = 2e5;
kp = 86;
rL = 1e3;
Sp = 250;

PiP = Sp*k5/(kp*k6);

% yp1 = dR/dt
% yp2 = dB/dt
```

```
% yp3 = dC/dt

yp1 = Dr*(CC+f0*Cs)/(CC+Cs)-f0*db/((CC+f0*Cs)/(CC+Cs))*RR;

yp2 = f0*db/((CC+f0*Cs)/(CC+Cs))*RR-kb*BB;

yp3 = Dc*(k3/k4)*((klp*PiP*BB)/(1+((k3*K)/(k4))+(k1/(k2*kO))*
    ((kop*RR/PiP)+IO))*(1+IL/rL))-Da*(CC+f0*Cs)/(CC+Cs)*CC;

yp = [yp1; yp2; yp3];

return
```

Appendix C

Code for Signaling Protein Model

```
function osteosign3(t, y)
format long

R0 = 7.7381e-004;
B0 = 7.2865e-004;
C0 = 9.1298e-004;
S0 = 0.999999999836619;
Q0 = 0.768185787811278;

Tstop = 120;
options = odeset('RelTol', 1e-9,'AbsTol', [1e-9 1e-9 1e-9 1e-12 1e-12]);
[T,Y] = ode45(@program5,0:0.01:Tstop, [R0 B0 C0 S0 Q0], options);

x1 = Y(:,1);
x2 = Y(:,2);
x3 = Y(:,3);
```

```
x4 = Y(:,4);
x5 = Y(:,5);

figure(1);clf;

plot(T, x1,'b');
xlabel('Time');
hold on;

plot(T, x2,'g');
xlabel('Time');

hold on;
plot(T, x3,'r');
xlabel('Time');
ylabel('Amount (pM)');

legend('Responding Osteoblasts','Active Osteoblasts','Active Osteoclasts');

figure(2);clf;
plot(T, x4,'y');
xlabel('Time');
ylabel('Signaling Protein');

figure(3);clf;
plot(T, x5);
xlabel('Time');
```

```
ylabel('PTH / Signaling Protein Complex');

x1(end);
x2(end);
x3(end);
x3(end)/x2(end)

return


function yp = program5(t,y)

RR=y(1);
BB=y(2);
CC=y(3);
SS=y(4);
QQ=y(5);

Cs = 5e-3;
Da = 0.7;
db = 0.7;
Dc = 2.1e-3;
Dr = 7e-4;
f0 = 0.05;
IL = 0;
IO = 0;
Ip = 0;
```

```
K = 10;
k1 = 10^-2;
k2 = 10;
k3 = 5.8e-4;
k4 = 1.7e-2;
k5 = 0.02;
k6 = 3;
kb = 0.189;
klp = 3e6;
kO = 0.35;
kop = 2e5;
kp = 86;
rL = 10^3;
Sp = 250;

% yp1 = dR/dt
% yp2 = dB/dt
% yp3 = dC/dt
% yp4 = dS/dt
% yp5 = dQ/dt

%P changes based on which method of PTH administration we are looking at
P= Sp/kp+350*sqrt(mod(t,1)).*exp(-37*mod(t,1)); %pulsed PTH administration
%P = Sp/kp + 350*sqrt(pi)/(2*37^(3/2)); %continuous PTH administration
%P=Sp/kp; %no PTH administration
PiP = P / (P+(k6/k5)-(Sp/kp));
kS=1.5;
```

```
kf=0.19;
kR=0.719;

lambda=150;
a=1/6;
b=5/6;

yp1 = Dr*(CC+f0*Cs)/(CC+Cs)-f0*db/((CC+f0*Cs)/(CC+Cs))*RR;

yp2 = f0*db/((CC+f0*Cs)/(CC+Cs))*RR-kb*exp(lambda*(SS-1))./(a+b*exp(lambda*(SS-1)))*BB;

yp3 = Dc*(k3/k4)*(klp*PiP*BB)/(1+((k3*K)/(k4))+(k1/(k2*kO))*
    ((kop*RR/PiP)+IO))*(1+IL/rL)-Da*(CC+f0*Cs)/(CC+Cs)*CC;

yp4 = kS*(1-SS)-kf*P*SS+kR*QQ;

yp5 = kf*P*SS-kR*QQ;

yp = [yp1; yp2; yp3; yp4; yp5];

return
```

Bibliography

[1] T. Bellido, A. Ali, L. Plotkin, Q. Fu, I. Gubrij, P. Roberson, R. Weinstein, C. O'Brien, S. Manolagas, and R. Jilka, *Proteasomal degradation of runx2 shortens parathyroid hormone-induced anti-apoptotic signaling in osteoblasts: A putative explanation for why intermittent administration is needed for bone anabolism*, The Journal of Biological Chemistry **278** (2003), 50259–50272.

[2] F. Cosman, N. Lane, M. Bolognese, J. Zanchetta, P. Garcia-Hernandez, K. Sees, J. Matriano, K. Gaumer, and P. Daddona, *Effect of transdermal teriparatide administration on bone mineral density in postmenopausal women*, The Journal of Clinical Endocrinology & Metabolism **95** (2010), 151–158.

[3] H. Dobnig and R. T. Turner, *Evidence that intermittent treatment with parathryoid hormone increases bone formation in adult rat by activation of bone lining cells*, Endocrinology **136** (1995), 3632–3638.

[4] David C. Dugdale, *Osteoporosis*, `http://www.nlm.nih.gov/medlineplus/ency/imagepages/17156.htm`, MAY 2009.

[5] J. Finkelstein, J. Wyland, B. Leder, S. Burnett-Bowie, H. Lee, H. Juppner, and R. Neer, *Effects of teriparatide retreatment in osteoporotic men and women*, The Journal of Clinical Endocrinology & Metabolism **94** (2009), 2495–2501.

[6] S. Komarova, *Mathematical model of paracrine interactions between osteoclasts and osteoblasts predicts anabolic action of parathyroid hormone on bone*, Endocrinology **146** (2005), 3589–3595.

[7] S. Komarova, R. Smith, J. Dixon, S. Sims, and L. Wahl, *Mathematical model predicts a critical role for osteoclast autocrine regulation in the control of bone remodeling*, Bone **33** (2003), 206–215.

[8] Martin H. Kroll, *Parathyroid hormone temporal effects on bone formation and resorption*, Bulletin of Mathematical Biology **62** (2000), 163–187.

[9] V. Lemaire, F. Tobin, L. Greller, C. Cho, and L. Suva, *Modeling the interactions between osteoblast and osteoclast activities in bone remodeling*, Journal of Theoretical Biology **229** (2004), 293–309.

[10] M. Peterson and M. Riggs, *A physiologically based mathematical model of integrated calcium homeostasis and bone remodeling*, Bone **46** (2010), 49–63.

[11] L. Potter, L. Greller, C. Cho, M. Nuttall, G. Stroup, L. Suva, and F. Tobin, *Response to continuous and pulsatile pth dosing: A mathematical model for parathyroid hormone receptor kinetics*, Bone **37** (2005), 159–169.

[12] J. Raposo, L. Sobrinho, and H. Ferreira, *A minimal mathematical model of calcium homeostasis*, The Journal of Clinical Endocrinology & Metabolism **87** (2002), 4330–4340.

[13] D.S. Ross, E. Agyingi, and K. Bathena, *A model of the transmission dynamics of leishmaniasis*, Journal Biological Systems **19** (2011), 237–250.

[14] D.S. Ross, C. Battista, A. Cabal, and K. Mehta, *Dynamics of bone cell signaling and pth treatments of osteoporosis*, Discrete and Continuous Dynamical Systems Series B (DCDS-B), in press.